Available online at www.sciencedirect.com
ScienceDirect
International Journal of Heat and Mass Transfer 51 (2008) 3378–3386
International Journal of HEAT and MASS TRANSFER
www.elsevier.com/locate/ijhmt

Hydrodynamic aspects of interaction between nucleation sites

R. Mosdorf [a,*], M. Shoji [b,1]

[a] Faculty of Computer Science, Bialystok University of Technology, 15-351 Bialystok, ul. Wiejska 45a, Poland
[b] Department of Mechanical Engineering, Kanagawa University, 3-27-1 Rokkakubashi, Kanagawa-ku, Yokohama, Kanagawa 221-8686, Japan

Received 1 November 2007
Available online 8 January 2008

Abstract

The dynamics of twin and triple nucleation sites interaction has been investigated. Nonlinear data analysis techniques such as the dimension spectrum and largest Lyapunov exponent have been used for analysis of data recorded in experiment. It has been shown that properties of dynamics of nucleation sites changes nonlinearly together with changing the spacing between cavities. To explain appearance of such properties of nucleation sites interaction the simulation of gas bubble movement in the liquid in the last stage of bubble departures has been made with using the stabilized finite element method and level set method. It has been shown that the bubble departure velocities and structure of velocity field around the bubbles nonlinearly depend on the initial horizontal spacing between bubbles. The obtained results indicate that one of the reasons for nonlinear changes of properties of dynamics of nucleation sites interaction occurring with changes of initial spacing between them is hydrodynamic interaction between departing bubbles.

Keywords: Pool boiling; Artificial surface; Boiling chaos; Nucleation site interaction

1. Introduction

Despite of the extensive study of boiling during the past over fifty years, the mechanism of nucleation sites interaction in nucleate boiling is still far from being fully understood due to the extreme complexity of the phenomena.

The relation between the bubble behaviors and the cavity spacing, S/D, has been studied experimentally by Chekanov [1], Calka and Judd [2], Gjerkeš and Golobic [3]. Several authors have studied the heat transfer characteristics of the artificial boiling surfaces with multiple cavities concerning applications to the cooling of highly integrated electronic devices [4,5]. Recently, by employing twin cavities, Zhang and Shoji [6], and triple cavities, Chatpun et al. [7,8], the mechanism of nucleation sites interaction has been investigated. The nonlinear analysis of temperature fluctuation at single and twin cavities, carried out by Mosdorf and Shoji, has been presented in the papers [9,10].

The analysis carried out in [9] has shown that properties of dynamics of nucleation sites such as correlation dimension and largest Lyapunov exponent change nonlinearly together with changing the spacing between cavities. The appearance of local minimum and maximum of correlation dimension and largest Lyapunov exponent has been observed. It has been distinguished two mechanisms of interaction between neighboring nucleation sites: hydrodynamic and thermal. The intensity of thermal interaction occurring inside the heating surface decreases with increase of the spacing between cavities. It seems that this process cannot be responsible for appearance of local minimum and maximum of correlation dimension and largest Lyapunov exponent that were observed in the experiment. Therefore we can assume that the hydrodynamic mechanism of interaction is responsible for such nonlinear changes of dynamics of nucleation sites. During different phases of bubble growth and its departure, the relation between the thermal and hydrodynamic processes changes. In many cases it is impossible to separate the thermal and hydrodynamic processes. But in

* Corresponding author. Tel.: +48 85 7422 041; fax: +48 85 7422 393.
E-mail addresses: mosdorf@ii.pb.bialystok.pl (R. Mosdorf), shoji@kanagawa-u.ac.jp (M. Shoji).
[1] Tel.: +81 45 481 5661x3371; fax: +81 45 481 5122.

0017-9310/$ - see front matter © 2007 Elsevier Ltd. All rights reserved.
doi:10.1016/j.ijheatmasstransfer.2007.11.023

Nomenclature

C	correlation coefficient
D	dimension, diameter of departing bubble, mm
d	distance in embedding dimension
f	bubble departure frequency, Hz
$\vec{g}$	acceleration of gravity, m/s^2
H	Heaviside's step function
L	largest Lyapunov exponent, bit/s
m	number of examined points
n	normal to interface
M	overall mass rate
N	samples number
p	pressure, Pa
q	heat flux, W/m^2
S	spacing between nucleation sites, mm
T	temperature, K
t	time of evolution, s
$\vec{u}$	velocity, m/s
v	vertical velocity, m/s
x	sample value, coordinate
y	coordinate

Greek symbols

ρ	density, kg/m^3
σ	surface tension, N/m
δ	Dirac delta function
φ	level set function
κ	curvature, 1/m
τ	time period, s, time delay
μ	viscosity, Pa s

Subscripts

2, 10,−10	correlation dimension indexes
g	gas
l	liquid

Superscript

k	iteration number

the last phase of bubble departure, when the phase change is not intensive and the coalescence does not appear, the hydrodynamic interaction between liquid flows generated by bubbles departing from neighboring cavities plays the important role. It seems that in this phase of nucleation sites interaction the thermal and hydrodynamic processes can be analyzed separately and properties of hydrodynamic interaction can be identified.

In the present paper, data recorded for triple cavities has been analyzed to study the dynamics of nucleation sites interaction. The nonlinear methods of analysis have been applied. The obtained results have been compared with results obtained in case of twin cavities interaction, that where presented in [9]. The hydrodynamic interaction between liquid flows generated by bubbles departing from neighboring cavities in the last phase of bubble departure has been modeled in the paper using the stabilized finite element method and level set method. The bubble and liquid velocities have been analyzed.

The obtained results show that one of the reasons for nonlinear changes of properties of dynamics of nucleation sites interaction occurring with changes of initial spacing between them is hydrodynamic interaction between departing bubbles.

2. Experimental setup

A 15 mm × 15 mm and 200 μm thick silicon disk with artificial nucleation sites was set as a test boiling surface inside the chamber filled with distilled water. A schematic view of the whole experimental setup is shown in Fig. 1. In the experiment, the vicinity of the manufactured cavity was heated by Nd-YAG laser irradiation (wavelength:1064 nm) from the bottom side of the test disk. The size of laser spot was 12 mm in diameter. The bottom surface of the disk was black oxide finished in order to improve absorptivity of the laser and emissivity from the surface. The temperature fluctuation just under the artificial cavity were recorded by radiation thermometer with spatial resolution of 120 μm, temperature resolution of

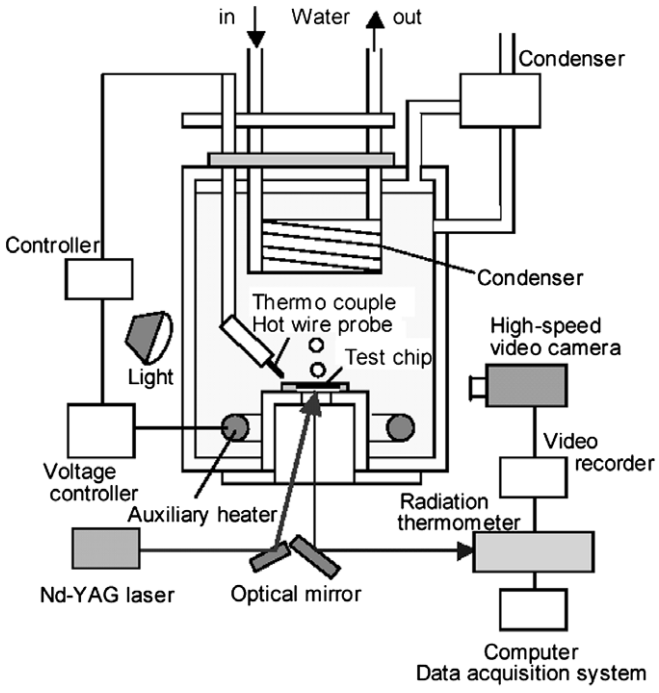

Fig. 1. Experimental apparatus.

0.08 K and time resolution of 3.0 ms. The corresponding bubbling status was recorded by high-speed video camera with the rate of 1000 frames/s. In this way, it was possible to measure temperature time series of cavity vicinity without any physical contact with the disk surface. The power of Nd-YAG laser was controlled to vary the heat input to the disk surface and was monitored by photo detector throughout the experiment. The distilled water at atmospheric pressure under saturated pool boiling condition was used as a working fluid. An acrylic fence was set inside the chamber to avoid effect of bubbling from auxiliary heater, which was activated during the experiment to maintain saturated boiling condition. The nucleation sites of 10 μm in diameter and 80 μm in depth were applied. In case of three nucleation sites the hot wire probe was located near the central nucleation site. The signals of hot wire probes were measured in voltage unit with time interval 0.001 s. Some results of data analysis from the experimental setup have been presented in the papers [7,9,10].

3. Selected methods of non linear data analysis

The trajectories of nonlinear dynamical system in the phase space form objects called strange attractors of the structure resembling the fractal. The analysis of strange attractor gives us information about the properties of dynamical system such as system complexity and its stability. The application of Takens theorem [11,15] – in connection with possibilities of modern measuring and computing techniques – enables an analysis of dynamics of non linear processes by analysis of single time series. In nonlinear analysis the reconstruction of attractor in certain embedding dimension has been carried out using the stroboscope coordination. In this method subsequent co-ordinates of attractor points have been calculated basing on the subsequent samples, between which the distance is equal to time delay τ. The time delay is a multiplication of time between the samples. For the measured data in the form of time series:

$$\{x_n\} = \{x_1, x_2, \ldots, x_n\} \tag{1}$$

the way of calculation of subsequent co-ordinates of points of attractor is shown in Fig. 2.

The dimension spectrum D_q is one of the essential characteristics of attractors, it allows us to identify the structure of attractors, especially the level of complexity of attractor versus attractor points density. It is defined by the following expression [12,15]:

$$D_q = \lim_{d\to 0} \frac{1}{\ln d} \ln C^q(d) \tag{2}$$

$$\text{where } C^q(d) = \left[\frac{1}{N}\sum_i \left(\frac{1}{N}\sum_j H(d - |x_i - x_j|)\right)^{q-1}\right]^{1/q-1} \tag{3}$$

The Heaviside's step function, H, determines the number of attractor's point pairs of the distance shorter than d. The parameter q indicates us for what density of attractor points the dimension is calculated. When $q \to -\infty$ then D_q characterizes the part of attractor with low density of points. When $q \to +\infty$ then dimension D_q characterizes the area of attractor with high density of points. When $q = 2$ then D_q is called the correlation dimension and is denoted by D_2. The dimension spectrum D_q estimates the number of freedom degrees of examined dynamical system which is responsible for creating the part of attractor with certain density of points. The correlation dimension D_2 characterizes the dimension of the entire attractor.

The another important characteristic of attractor is the largest Lyapunov exponent. In this case two points on the attractor immersed in D dimensional space have been selected. The distance between these two points $d(t_j)$ should be equal at least to one orbiting period. After the passage of some evolution time the distance of selected points has been calculated again and denoted as $d(t_{j+1})$. The largest Lyapunov exponent has been calculated according to the formula [13]:

$$L = \frac{1}{t}\sum_{j=1}^{m} \log_2 \frac{d(t_{j+1})}{d(t_j)} \tag{4}$$

The largest Lyapunov exponent allows us to calculate the time period of long time memory in the system, $(1/L)$, in which the process of stability loss occurs. The increase in $(1/L)$ means that the process becomes more predictable. The comparison between the value of long time memory calculated from the largest Lyapunov exponent, $1/L$, and the average time interval between departing bubbles, $1/f$, allows us to estimate the stability of bubble departures. The value of $(1/L - 1/f)/(1/f)$ defines the number of subsequent bubbles in the series in which the behaviors of first and last bubble are independent.

Embedding dimension (subsequent coordinates)

Point number	1	2	3	4	5	6	
1	x_1	$x_{1+\tau}$	$x_{1+2\tau}$	$x_{1+3\tau}$	$x_{1+4\tau}$	$x_{1+5\tau}$	...
2	x_2	$x_{2+\tau}$	$x_{2+2\tau}$	$x_{2+3\tau}$	$x_{2+4\tau}$	$x_{2+5\tau}$	...
3	x_3	$x_{3+\tau}$	$x_{3+2\tau}$	$x_{3+3\tau}$	$x_{3+4\tau}$	$x_{3+5\tau}$	...
4	x_4	$x_{4+\tau}$	$x_{4+2\tau}$	$x_{4+3\tau}$	$x_{4+4\tau}$	$x_{4+5\tau}$	...
5	x_5	$x_{5+\tau}$	$x_{5+2\tau}$	$x_{5+3\tau}$	$x_{5+4\tau}$	$x_{5+5\tau}$	...
6	x_6	$x_{6+\tau}$	$x_{6+2\tau}$	$x_{6+3\tau}$	$x_{6+4\tau}$	$x_{6+5\tau}$	...
...	...	...	...	...	...	...	...

Fig. 2. Time delay algorithm of calculation of attractor co-ordinates.

4. Dynamics of nucleation sites interaction

4.1. Two nucleation sites interaction

In the paper [9] two following mechanisms of interaction between neighboring nucleation sites: the hydrodynamic one occurring over the heating surface and thermal one occurring inside the heating surface have been identified and discussed. It has been demonstrated that the attractor created from temperature fluctuation at single nucleation site has a triangle shape. The correlation dimension of this

attractor is equal to 3.7 and the largest Lyapunov exponent is equal to ≈30 bit/s. The time of long time memory ($1/L$) is close to time of bubble departure. This means that: four-dimensional system is enough sophisticated to describe the bubble departures from single nucleation site and the process of stability loss of bubble departures occurs approximately in time interval equal to average time interval of single bubble growth [9].

In case of two nucleation sites interaction [9], when the distance between the nucleation sites increases, the shape of one of sections of attractor is also similar to the triangle, but in the direction perpendicular to this section the shape becomes more complex. The complexity of the system increases and the time of long time memory becomes much greater than the time interval between subsequent bubbles. The analysis of temperature changes at the nucleation site shows that interaction processes are responsible for creating the part of attractor with low density of points. Therefore the dimension D_{-10} has been used to identify the complexity of mechanisms of interactions between the nucleation sites. The dimension D_{-10} and largest Lyapunov exponent have been presented in Fig. 3 and compared with bubble departure frequency.

The maximum and minimum of D_{-10} identify spacing for which the dynamics of interaction qualitatively changes. For $1.1 < S/D < 2$ the increase of initial spacing between bubbles causes the increase of interaction mechanism complexity. This process is connected with decrease of interaction what causes that cavities become independent and finally the number of freedom degrees of the system increases. For $1 < S/D < 1.1$ the increase of initial spacing between bubbles causes the decrease of interaction mechanism complexity. It happens because in this range the interaction increases (because of small distance between bubbles) and behavior of two cavities (considered together) becomes similar to behavior of single cavity. For $S/D > 2$ the increase of initial spacing between bubbles causes the decrease of interaction mechanism complexity. It happens because the cavities become independent and behavior of each cavity is similar to behavior of single cavity.

The comparison of bubble departure frequency, f, and long time memory, $1/L$, (Fig. 3) has shown that for $S/D \approx 0.63$ and $S/D \approx 2.5$ on the one hand the bubbles are promoted to departure but on the other hand the bubble departures become more predictable. For $S/D > 3$ the nucleation sites become independent and the frequency of bubble departure decreases. The local maximums of dimension D_{-10}, $1/L$ and bubble departure frequency, f, appear for the same value of S/D.

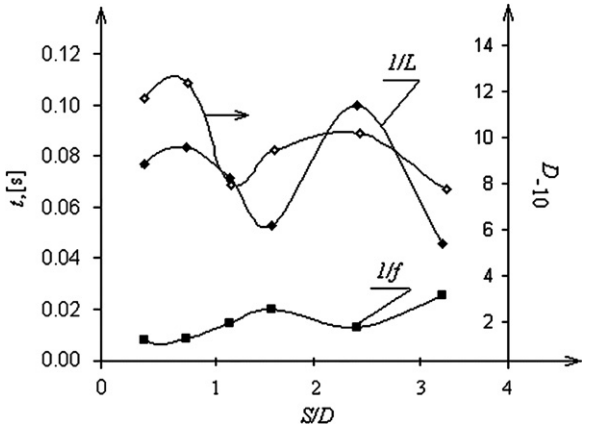

Fig. 3. The nonlinear analysis of temperature changes at nuclearion site in twin cavities systems for $q = 26.5$ [kW/m^2] [9]. The correlation dimension has been calculated according to algorithm Grassberger P., Procaccia I. [12], the largest Lyapunow exponent has been calculated using the Wolf algorithm [13].

4.2. Three nucleation sites interaction

In this paper the linear configuration of three nucleation sites has been considered. In this experiment the mean diameter of departing bubble was equal to 1.7 mm [7,8]. In Fig. 4 typical behavior of bubble emission from the triple nucleation sites for different bubble spacing S/D has been presented. In Fig. 4a–c we can observe the process of coalescence of bubbles departing from three neighboring nucleation sites. In Fig. 4d the bubbles interact only by liquid flow generated by bubbles.

In Fig. 5a it has been shown the process of large bubble formation for $S/D = 0.59$. The time between the frames is equal to 0.004 s. The growth of three small bubbles is visible in Fig. 5, in the frame 3. After the coalescence of two bubbles (central and left) with previously departed large bubble (frame 4, Fig. 5a), the new large bubble created in such a way is rapidly growing, dividing and departing (frame 5, Fig. 5a). The remaining small bubbles are coalescing and the process of large bubble growth is starting again (frame 6, Fig. 5a).

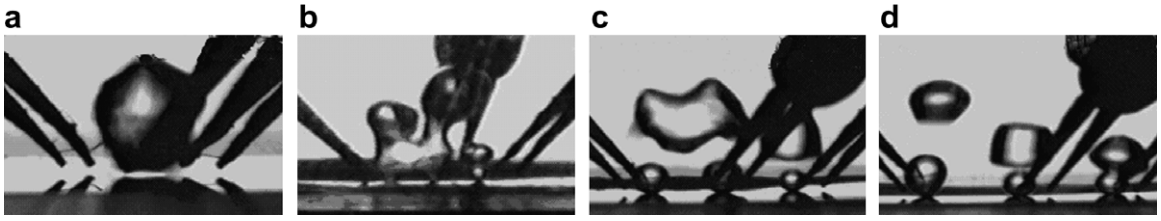

Fig. 4. The typical behavior of bubble emission from the triple nucleation sites for q=39.5 kW/m^2 and different spacing between the nucleation sites. (a) $S/D = 0.59$, (b) $S/D = 1.18$, (c) $S/D = 1.76$, (d) $S/D = 2.35$. Time spacing between frames is 4 ms.

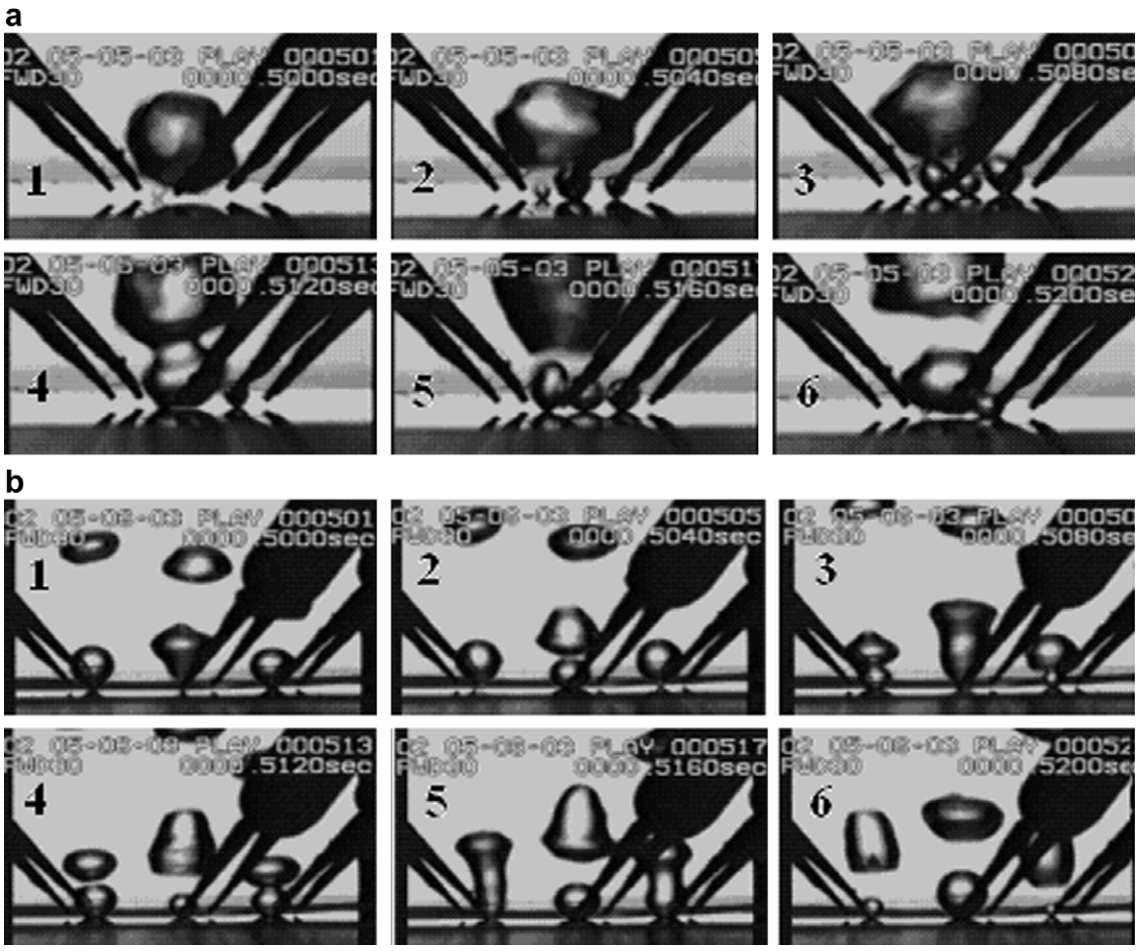

Fig. 5. The behavior of bubble emission from triple nucleation sites $q = 39.5\ \mathrm{kW/m^2}$. (a) $S/D = 0.59$, (b) $S/D = 2.35$. Time spacing between frames is 4 ms.

In Fig. 5b it has been shown the formation of the bubble over the central nucleation site. Two subsequent departing bubbles are vertically coalescing (frame 2 and 3, Fig. 5b) and then they are creating the large bubble that is departing in the frame 4, in Fig. 5b. Neighboring bubbles (left and right) are growing at the same rate. In situation shown in Fig. 5b the central bubble is like 'symmetry axis'.

In Fig. 6 the dimension D_{-10} of attractor obtained from temperature fluctuation at central nucleation site has been compared with dimension D_{-10} calculated in case of twin nucleation sites.

For $S/D < 1.1$ the dynamics of three interacting sites is less complex in comparison with dynamics of twin nucleation sites interaction. The opposite situation is observed for $S/D > 1.1$ when the interaction by liquid flow between three nucleation sites is more complex than interaction between two nucleation sites. In case of three nucleation sites for small distance between neighboring cavities the behavior of central cavity becomes similar to single cavity. Similarly, like in case of twin cavities, the complexity of interaction changes nonlinearly together with decrease of spacing between cavities. The local maximum of dimension D_{-10} is observed almost for the same value of S/D as in case of twin cavities. The increase of the heat flux supplied

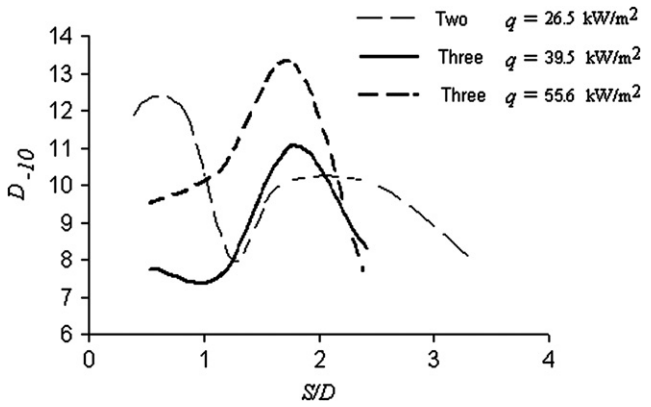

Fig. 6. The dimension D_{-10} of attractors created from temperature fluctuation in case of twin and triple nucleation sites interaction.

to the heating surface causes the increase of system complexity. For $q = 39.5\ \mathrm{kW/m^2}$ the local minimum of D_{-10} is also observed.

In Fig. 7 it has been shown the time of long time memory, $1/L$, obtained for data from the hot wire probe located near the central nucleation site. The results have been compared with results obtained from temperature fluctuation and bubble departure frequency. The comparison shows

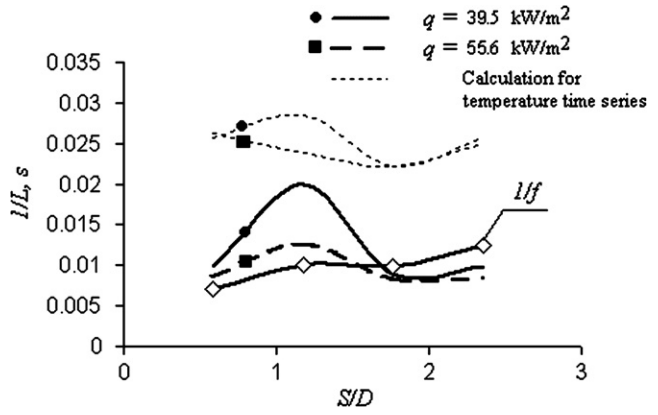

Fig. 7. Time of stability loss obtained for data from hot wire probe and temperature fluctuation for triple cavity in linear model. The bubble departure frequency, f, has been recorded for heat flux equal to 50.4 kW/m^2.

that hydrodynamic processes occurring during the bubbles interaction are more instable compared to thermal processes. For $S/D > 1.7$ the time of stability loss of hydrodynamic processes is close to average time between departing bubbles.

In case of three cavities the largest Lyapunov exponent also changes nonlinearly together with increase of spacing between cavities. The bubble departure frequency reaches the local minimum for $S/D = 1.1$. In this case the process of bubble departure becomes more stable, contrary to the case of twin nucleation sites.

5. Modeling of hydrodynamic interaction of departing bubbles

The nonlinear analyses carried out in the paper [9] allow us to distinguish two mechanisms of interaction between neighboring nucleation sites: hydrodynamic one occurring over the heating surface and thermal one occurring inside the heating surface. Generally we can say that interaction between the nucleation sites through the liquid stabilizes the processes of bubble growth and its departure, while the thermal interaction destabilizes these processes.

The analyses have shown that correlation dimension and largest Lyapunov exponent change nonlinearly together with changing the spacing between cavities. The appearance of local minimum and maximum of correlation dimension and largest Lyapunov exponent has been observed. It seems that thermal interaction between cavities occurring inside the heating surface can not be responsible for appearance of local minimum and maximum of correlation dimension and largest Lyapunov exponent that where observed in the experiment. The separation of thermal and hydrodynamic processes occurring during the growth and departure of bubbles is difficult. But in the last phase of bubble departure, when the phase change is not intensive and the coalescence does not appear, the hydrodynamic interaction between liquid flows generated by bubbles departing from neighboring cavities plays the important role. It seems that in this phase of nucleation sites interaction the thermal and hydrodynamic processes can be analyzed separately and properties of hydrodynamic interaction can be identified. In this chapter the last phase of bubble departure, when the phase change is not intensive and the coalescence does not appear, the hydrodynamic interaction between liquid flows generated by bubbles departing from neighboring cavities has been modeled. The simulation of gas bubble movement in liquid has been made with using the stabilized finite element method and level set method. The time-dependent COMSOL Multiphysics solver [14] with streamline diffusion (Petrov-Galerkin/Compensated, tuning parameter equal to 0.25) has been used for solving 2D Navier-Stokes equations [14]:

$$\rho\left(\frac{\partial \vec{u}}{\partial t} + \vec{u}\cdot\nabla\vec{u}\right) - \nabla\cdot\left[\mu(\nabla\vec{u} + \nabla\vec{u}^T)\right] + \nabla p = \sigma\kappa\vec{n}\delta + \rho\vec{g}$$
$$\nabla\cdot\vec{u} = 0 \tag{5}$$

In the level set method the zero level set at $\phi = 0$ determines the position of the interface. The changes in time of level set function ϕ have been described by the following equation [16,17]:

$$\frac{\partial\varphi}{\partial t} + \vec{u}\cdot\nabla\varphi = 0 \tag{6}$$

In the simulation the fluid density has been described by the following equation [14,16]:

$$\rho = \rho_g + H(\varphi)\cdot(\rho_l - \rho_g) \tag{7}$$

$$\text{where} \quad H(\varphi) = \begin{cases} 0 & \text{if} \quad \varphi < 0 \\ 1 & \text{if} \quad \varphi > 0 \end{cases}$$

Under the evolution of Eq. (6), the values of the level set function that are close to zero may move with velocities different than those of the zero values of level set function. Therefore, the ϕ distance field gets distorted ($|\nabla\varphi|$ becomes different than 1). In this case the gas volume changes during the simulation. The re-initialization of the level set function in regular intervals in order to rebuild the signed distance function is necessary. The direct application of re-initialization procedure in the Comsol solver is difficult because of their small ability to modification of solving procedure. Therefore the Comsol proposes a slight modification of Eq. (6) by adding the diffusion at the interface to maintain the bubble volume during the simulation. Finally, the following equation:

$$\frac{\partial\varphi}{\partial t} + \vec{u}\cdot\nabla\varphi = \delta(\varphi)\cdot\nabla\cdot(D\nabla\varphi) \tag{8}$$

has been solved instead of Eq. (6) [14].

The important factor in monitoring a level set simulation is the total mass. The integral of the mass over the domain as a function of time indicates the mass conservation during the simulation. The value of coefficient D has been set in such a way that the overall mass rate [14]:

$$M = \int \rho(t)\mathrm{d}x\mathrm{d}y / \int \rho(t_0)\mathrm{d}x\mathrm{d}y, \tag{9}$$

reaches the minimum. During the simulation the overall mass rate increases and the constant value of coefficient D can not compensate this increase, therefore the simulation has been carried out in time period of 0.05 s, for which the assumed accuracy $M < 0.1\%$ has been reached.

The simulation has been made for air and water: $\rho_l = 1000\ \mathrm{kg/m^3}$, $\rho_g = 1\ \mathrm{kg/m^3}$, $\sigma = 0.07$ N/m, $g = 10\ \mathrm{m/s^2}$, $\mu = 0.075$ Pa s. The two dimensional air bubbles flow in tank (40 mm × 15 mm) filled with water has been considered. The area of container has been divided into square elements (30 × 80). The velocity and pressure has been set to zero at $t = 0$. Boundary settings: no-slip conditions, $u = 0$, have been used on boundary of liquid container.

When at the beginning of simulation the bubble wall touches the bottom of the tank, then during the next stages of simulation the bubble becomes elongated. This happens because the liquid velocity on the wall of the tank is equal to zero. This situation is similar to bubble detachment from the nozzle, orifice or nucleation site. The examples of evolution of twin and triple bubbles are shown in Fig. 8. Bubbles departing from the bottom of the tank generate the liquid flows shown in Fig. 8, where the velocity field and shape of bubbles for $t = 0.05$ s have been shown. The results of simulation show that the liquid velocity between departing bubbles depends on initial bubble spacing. When this spacing is small (Fig. 8c and d), the liquid between bubbles moves up the tank. When the spacing increases (Fig. 8a and b), the liquid moves down the tank.

In Fig. 9 the bubble velocities and liquid velocity between them have been shown as the function of S/D. The liquid velocity has been recorded 4 mm above the tank bottom at $t = 0.05$ s while the bubble velocity was recorded at the same time as the velocity of top of the bubble. For two bubbles for $S/D \leqslant 1.2$ and for three bubbles for

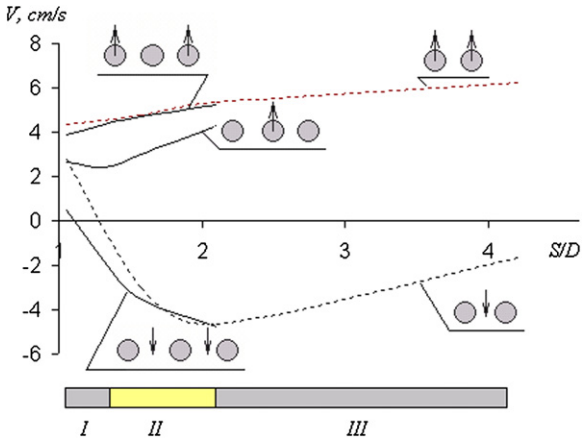

Fig. 9. The liquid and bubble velocities changes against the cavity spacing. Velocity has been recorded for $t = 0.05$ s and initial bubble diameter was $D = 3.8$ mm.

$S/D \leqslant 1.1$ the liquid velocity between bubbles has a positive value, it means that the liquid moves up. For $S/D > 1.1$ (three bubbles) and $S/D > 1.2$ (two bubbles) the liquid velocity between bubbles has a negative value, it means that liquid moves down. This negative velocity reaches the minimum negative value for $S/D = 2$. For $S/D > 4$ the liquid velocity between bubbles become close to zero.

In Fig. 9 the vertical velocity of bubbles against bubble spacing has been shown as well. In the cases of two bubbles and three bubbles (left and right bubbles) the increase of initial bubble spacing causes the increase of their velocity. In case of three departing bubbles the vertical velocities of left and right bubbles are greater than velocity of the central bubble.

The vertical bubble movement generates at both sides of bubble the liquid flow in direction of tank bottom. In case of two departing bubbles the liquid flow down between bubbles is modified because of vertical movement of interacting bubbles. In this case the kinetic energy of bubbles is

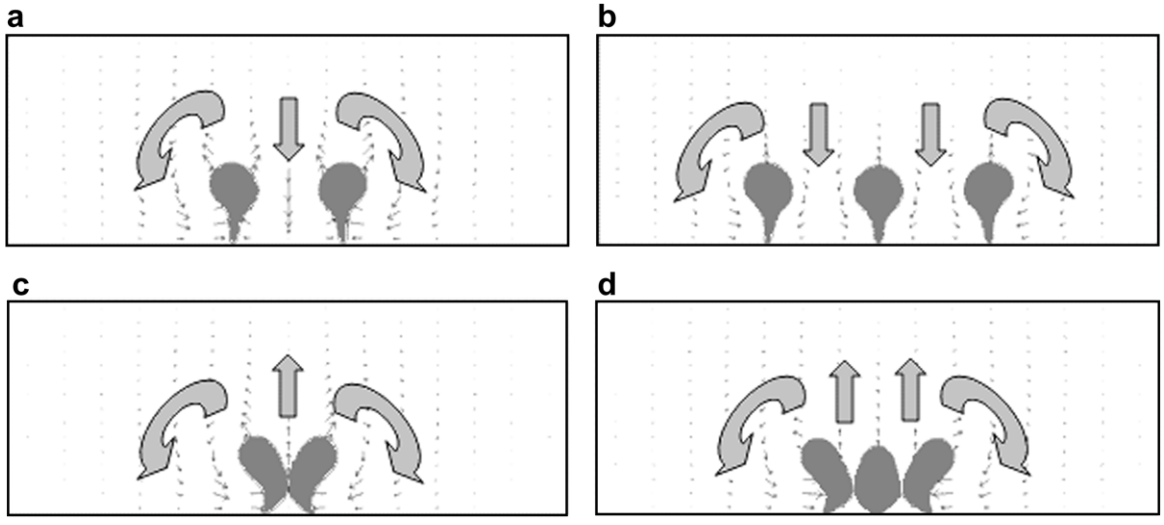

Fig. 8. Twin and triple bubble evolution. The shape of the bubbles and liquid velocity field around the bubbles for $t = 0.05$ s and different bubble spacing. (a), (b) $S/D = 2.1$, (c), (d) $S/D = 1.05$.

used to decreasing the velocity of liquid flow down between bubbles. This process decreases the vertical velocity of departing bubbles for low values of S/D, as it has been shown in Fig. 9.

The computer simulations show that liquid flow between departing bubbles decreases the vertical bubble velocities. Such behavior of departing neighboring bubbles may result in decrease of bubble departure frequency (for small distance of cavities) that was observed in the experiment. The change of the direction of vertical liquid velocity between bubbles (in computer simulation) indicates the ranges of S/D where velocity field around departing bubbles has different qualitative character. Such ranges have been schematically shown in Fig. 9. In the first range (I) the liquid between bubbles flows in the same direction as bubbles. In the second range (II) the liquid between bubbles moves in the direction of tank bottom. In this range, when spacing between bubbles increases, the value of liquid velocity between bubbles increases as well. In the third range (III) the liquid between bubbles also moves in the direction of tank bottom but when spacing between bubbles increases, the value of liquid velocity between bubbles decreases. The appearance of such three ranges characterized by different structures of liquid flow around departing bubbles may be one of the reason for appearance of nonlinear changes of correlation dimension and largest Lyapunov exponent with changes of distance between cavities.

6. Conclusions

The analysis of behavior of twin and triple nucleation sites interaction can be concluded as follows:

6.1. For twin nucleation site

The change of initial bubble spacing leads to nonlinear change of bubble departure frequency and stability of the bubble departures ($1/L$). Together with the increase of frequency of bubble departures the complexity and stability of system increase. Bubble departures become the most instable for $S/D = 1.5$, in this case the bubble departure frequency reaches the local minimum.

6.2. For triple nucleation sites

The dynamics of temperature changes under the large bubble (for $S/D < 1$) is less complex in comparison with dynamics of temperature changes in case of twin nucleation sites. The dynamics of liquid movement is the simplest for $S/D = 1.1$. Also for this spacing, the bubble departures become more predictable and frequency of their departures reaches the local minimum.

The computer simulation of hydrodynamic interaction of departing bubbles can be concluded as follows:

During the bubble departures we can distinguish at least three liquid flow regimes. In the first one, after an initial phase of bubble departure the liquid is moved up from the space between bubbles. In the other one, the liquid moves down in the space between bubbles. The minimum value of liquid velocity defines the end of second region and beginning of third region. The minimum of bubble departure frequency has been observed in the experiment almost for the same value of S/D like minimum velocity of bubble departure in simulation.

The computer simulation shows that for small distance between bubbles their departure velocity decreases. In case of three departing bubbles the liquid velocities at the both sides of central bubble are the same. This situation seems to be more stable compared with two departing bubbles, where at the both sides of each of bubbles the different liquid velocities occur.

Acknowledgement

The authors would like to express their appreciation to Dr. Lei Zhang and Ms. Chatpun Surapong for their continuous discussion and contribution in performing the experiment.

References

[1] V.V. Chekanov, Interaction of centers in nucleate boiling, Teplofzika Vysokikh Temperaur 15 (1977) 121–128.
[2] A. Calka, R.L. Judd, Some aspects of the interaction among nucleation sites during saturated nucleate boiling, Int. J. Heat Mass Transfer 28 (1985) 2331–2342.
[3] H. Gjerkeš, I. Golobic, Measurement of certain parameters influencing activity of nucleation sites in pool boiling, Exp. Therm. Fluid Sci. 25 (2002) 487–493.
[4] H. Kubo, H. Takamatsu, H. Honda, Effects of size and number density of micro-reentrant cavities on boiling heat transfer from a Silicon chip immersed in degassed and gas-dissolved FC-72, Enhanced Heat Transfer 6 (1999) 151–160.
[5] S.H. Bhavnani, G. Fournelle, R.C. Jaeger, Immersion-cooled heat sinks for electronics: insight form high-speed photography, IEEE Trans. Comp. Packag. Technol. 23 (2001) 166–176.
[6] L. Zhang, M. Shoji, Nucleation site interaction in pool boiling on the artificial surface, Int. J. Heat Mass Transfer 46 (2003) 513–522.
[7] Surapong Chatpun, Makoto Watanabe, Masahiro Shoji, Experimental study on characteristics of nucleate pool boiling by the effects of cavity arrangement, Exp. Therm. Fluid Sci. 29 (2004) 33–40.
[8] Surapong Chatpun, Makoto Watanabe, Masahiro Shoji, Nucleation site interaction in pool nucleate boiling on a heated surface with triple artificial cavities, Int. J. Heat Mass Transfer 47 (2004) 3583–3587.
[9] R. Mosdorf, M. Shoji, Chaos in nucleate boiling – nonlinear analysis and modelling, Int. J. Heat Mass Transfer 47 (6–7) (2004) 1515–1524.
[10] M. Shoji, R. Mosdorf, L. Zhang, Y. Takagi, K. Yasui and M. Yokota, Features of boiling on an artificial surface – bubble formation, wall temperature fluctuation and nucleation site interaction, in: First International Symposium on Thermal Science and Engineering, Beijing, China, October 23–26, 2002, pp. 293–302.
[11] H.G. Schuster, Deterministic Chaos an Introduction, Physik-Verlag GmbH, Weinheim, 1984.
[12] P. Grassberger, I. Procaccis, Measuring the strangeness of strange attractors, Physica D 9 (1985) 189–208.
[13] A. Wolf, J.B. Swift, H.L. Swinney, J.A. Vastano, Determining Lyapunov exponent from a time series, Physica-D 16 (1985) 285–317.
[14] Comsol Multiphysics. Rising Bubble Modeled with the Level Set Method solved with Comsol Multiphysics 3.2. <http://www.comsol.com/showroom/gallery/177.php?highlight=bubble>.

[15] K. Pawelzik, H. Schouster, Generalized dimension and entropies from a measured time series, Phys. Rev. A (Rapid Commun.) 35 (1) (1987) 481–483.
[16] Sunitha Nagrath, Kenneth E. Jansen, Richard T. Lahey, Three dimensional simulation of incompressible two-phase flows using a stabilized finite element method and a level set approach. (Preprint).
[17] Petter Andreas Berthelsen, A short introduction to the level set method and incompressible two-phase flow, a computational approach, 2002 NTNU document, December 2002. <http://www.petronics.ntnu.no/publications/berthelsen/berthelsen_report2002.pdf>.